# FEASIBILITY STUDY ON THE *IN-SITU* MEASUREMENTS OF THE VELOCITY DISTRIBUTION FUNCTION OF THERMAL IONS IN THE POLAR IONOSPHERE

Eiichi SAGAWA[1] and Hirotaka MORI[2]

[1]*Radio Research Laboratories, 2–1, Nukui-Kitamachi 4-chome, Koganei-shi, Tokyo 184*
[2]*Hiraiso Branch, Radio Research Laboratories, 3601, Isozaki, Nakaminato 311–12*

***Abstract:*** It has been proposed that *in-situ* measurements of the velocity distribution functions of thermal ions in the polar ionosphere give various information of the ionospheric plasma such as the plasma drift velocities, ion temperatures, ion number densities, and existence of ion beam in the suprathermal energy region. Several works have reported the promising results of the ion distribution function measurements in the auroral ionosphere by using the electrostatic energy analyzers onboard sounding rockets. Basic considerations on this method of measurements are reviewed with discussions about the effects of the rocket potential and wake. A preliminary test is carried out in the laboratory plasma to demonstrate the capability of this technique. Finally, an instrumentation is proposed for a sounding rocket experiment at the antarctic station.

## 1. Introduction

It is established that the coldest part of the ionospheric ions is well described by the drift Maxwell-Boltzman distribution having ion temperature of about 0.1 eV. *In-situ* measurements of the ion distribution functions in the three-dimensional (3-D) phase space will give the plasma drift velocity, ion temperature and other useful information, for example, the suprathermal part of the ion distribution functions which is important when strong interactions between particles and plasma waves occur. The measurements of the distribution functions have been widely utilized in the study of the magnetospheric hot plasma in order to determine its temperatures and drift velocities. The same technique can be, basically, applicable to the study of the ionospheric plasma except for some practical problems due to the vehicle potential which is comparable to or larger than the mean particle energy.

Langmuir probes and retarding potential analyzers (RPA) have long been used to measure directly the energy distribution of the thermal plasma in the ionosphere. The technique utilizing an electrostatic energy analyzer (ESA) has some advantages over those. First, the ESA has a narrow and well-defined field of view while RPA and Langmuir probe have a very wide and poorly-defined field of view. This point makes the ESA suitable for the 3-D measurements by scanning its direction over a wide range of solid angle. Second, electrodes of the ESA to which the sweep voltage is applied in order to vary the energy of the ions to be selected do not have a direct contact with the ambient plasma. Therefore, the effects due to the surface contamination which is a serious problem in the measurements by RPA and Langmuir probe are not considered important in the case of the ESA. On the other hand, a shortage in sensitivity arises from its narrow field of view. To resolve this problem, the ESA must be equipped with a high sensitive particle detector such as a channel electron multiplier (CEM).

From the viewpoint of the ion drift measurements, an instrument similar to RPA onboard AE satellites was successful as described by HANSON and HEELIS (1975). However, because this instrument makes use of the shadow of the entrance aperture projected onto its divided collectors in order to measure the angle of the incoming plasma flow relative to the satellite velocity vector, it may not work well on a sounding rocket where the vehicle velocity is close to the mean thermal speed of ions. In contrast, the vehicle velocity is not essential to the drift measurements by the ESA even though a large difference among magnitudes of velocities of the vehicle, thermal motion, and plasma drift makes the measurements difficult. Fortunately those are of the same order of magnitude in the case of a sounding rocket observation in the polar $F$ layer.

WHALEN *et al.* (1974) first tried to measure directly the ion distribution functions by using the ESA onboard the sounding rocket. They used a single ESA whose field of view is directed perpendicular to the rocket spin axis so that the 2-D distribution functions were obtained every one spin period. Moreover, the coning motion of the rocket allowed them to obtain the plasma drift velocities parallel and perpendicular to the local geomagnetic field. They have found that the observed perpendicular velocity is close to that expected from the convective electric field measurements. An interesting result of their experiments is a strong upward field-aligned ion flow having a good correlation with the electron precipitations measured on the same rocket. It is one of unique capabilities of this technique to be able to measure the parallel velocity of plasma which the double probe technique may not be able to provide.

Comparisons of measurements of the perpendicular electric field by several techniques have been carried out by MORGAN and ARNOLDY (1978) and ZANETTI *et al.* (1980). Their attempts have shown that this technique gives reasonable results in view of the electric field measurements in addition to other important information that it can provide.

In this report, principle of this technique is first described with considerations on the effects of the vehicle potential and wake. Then an attempt to measure the ion distribution functions of the laboratory plasma is accompanied by a proposal of the rocket experiment at the antarctic station.

## 2. Principle

For an ESA with a narrow field of view, the relationships among the directional differential energy flux ($J(E)$), 3-D velocity distribution function ($f(V)$), and counts of CEM during $\Delta t$ second ($N(E)$) are approximately given by eq. (1), if $J(E)$ changes little within the ESA's energy pass band ($\Delta E$) and field of view. This is a valid assumption except for the lowest energy part of the distribution function where $N(E)$ should be expressed by the convolutional integral of the incoming particle flux with the instrument response function over $\Delta E$ and the field of view.

$$J(E)=\frac{2E}{m^2}f(V)=\frac{N(E)}{G_0 \Delta t E}\ , \tag{1}$$

where $m$ is the particle mass, $E$ and $V$ are the particle energy and velocities parallel to the sensor direction, respectively, and $G_0$ is the geometrical factor of the ESA in $cm^2$ sr eV/eV. Equation (1) neglects the effects of the vehicle potential relative to the surrounding plasma which is typically about one volt in the $F$ layer. If the vehicle is charged at $\Delta U$ volt negative, the total energy $E'$ measured at the ESA increases by $q\Delta U$,

$$E'=E+q\Delta U\ , \tag{2}$$

where $q$ is the charge of ion. Measured differential energy fluxes $J'(E')$ are connected with actual fluxes $J(E)$ by Liouville's theorem,

$$\frac{J'(E')}{E'}=\frac{J(E)}{E}\ . \tag{3}$$

When a drift Maxwell-Boltzman distribution is substituted into eq. (3),

$$J'(E')=\frac{2nE'}{m^2}\left[\frac{m}{2\pi kT}\right]^{2/3}\exp\left\{-\frac{m(V-V_0)^2}{2kT}\right\}\ , \tag{4}$$

where $n$ and $T$ are the plasma number density and temperature, $V$ is the particle velocity outside the sheath ($|V|=(2(E'-q\Delta U)/m)^{1/2}$), and $V_0$ is the bulk velocity of the plasma seen from the vehicle in motion. $V_0$ can be expressed as follows,

$$\boldsymbol{V}_0=\frac{\boldsymbol{E}\times\boldsymbol{B}}{B}+\boldsymbol{V}_{\parallel}-\boldsymbol{V}_r\ , \tag{5}$$

where $\boldsymbol{E}$ and $\boldsymbol{B}$ are the ionospheric electric and magnetic fields, respectively, $\boldsymbol{V}_r$ is the vehicle velocity, and $\boldsymbol{V}_{\parallel}$ is the plasma drift along $B$. Acceralation of ions through the sheath reduces actually the energy resolution with the decrease of $E'$. The flux of the particles having the energy of $E_1$ eV outside the sheath is measured at $E_1+q\Delta U$ volt inside the sheath where the ESA's energy pass band is given by $(E_1+q\Delta U)R$ by using the ESA's resolution $R$ which is independent of the selected energy. Therefore, in order to determine the precise form of the distribution function in the lowest energy range, roughly up to about $q\Delta U$ eV, from $N(E')$, $J(E')$ needs to be calculated by means of a deconvolution with the instrument response function instead of eq. (1).

By using the measured $N(E')$ in the energy range where eq. (4) gives a good approximation to the energy distribution of the ionospheric plasma, a non-linear least squares fit to this equation provides the six parameters ($V_0$, $T$, $\Delta U$, $n$). If a discernible deviation from the Maxwell-Boltzman distribution exists in the data, it should be treated separately. But even in this case, the main body of the energy distribution is expected to be described well by eq. (4), and the suprathermal part of the distribution functions may add some important information.

In addition to the energy shift discussed above, the sheath causes the ESA to have energy dependence of its field of view. Particles entering the sheath obliquely are focused onto the enterance aperture due to acceralation in it. But this effect has been calculated to be important only for particles with the lowest energy by GREEN and WHALEN (1974) and MORGAN and ARNOLDY (1978).

Another important point to be discussed here is the effects of the vehicle wake which is inevitably produced behind the vehicle body moving in the plasma with a super-sonic speed. As the nature of the plasma in the wake is much different from the natural one and is very disturbed, particles having passed through the wake must be excluded in the data analysis. Owing to larger Larmor radii of ions than sizes of the rocket, trajectories of ions are approximated well by straight lines. Therefore it is sufficient to avoid the wake effect that the data are discarded when the entrance aperture of the ESA is directed to the wake.

## 3. Laboratory Tests

An objective of this laboratory experiment is to test the operation of an ESA in the environment similar to the ionosphere. Figure 1 shows schematically the experimental setup. The ESA employed is a type of quadrispherical electrostatic energy analyzer with a CEM. Even though this type of ESA has a fan-shaped field of view and can resolve the arrival angle of the incoming particles, only a central part of the field of view is used in this experiment. A type of Multi-dipole Plasma Source (MPS) has a large number of small dipole magnets at its wall in order to increases the ioniza-

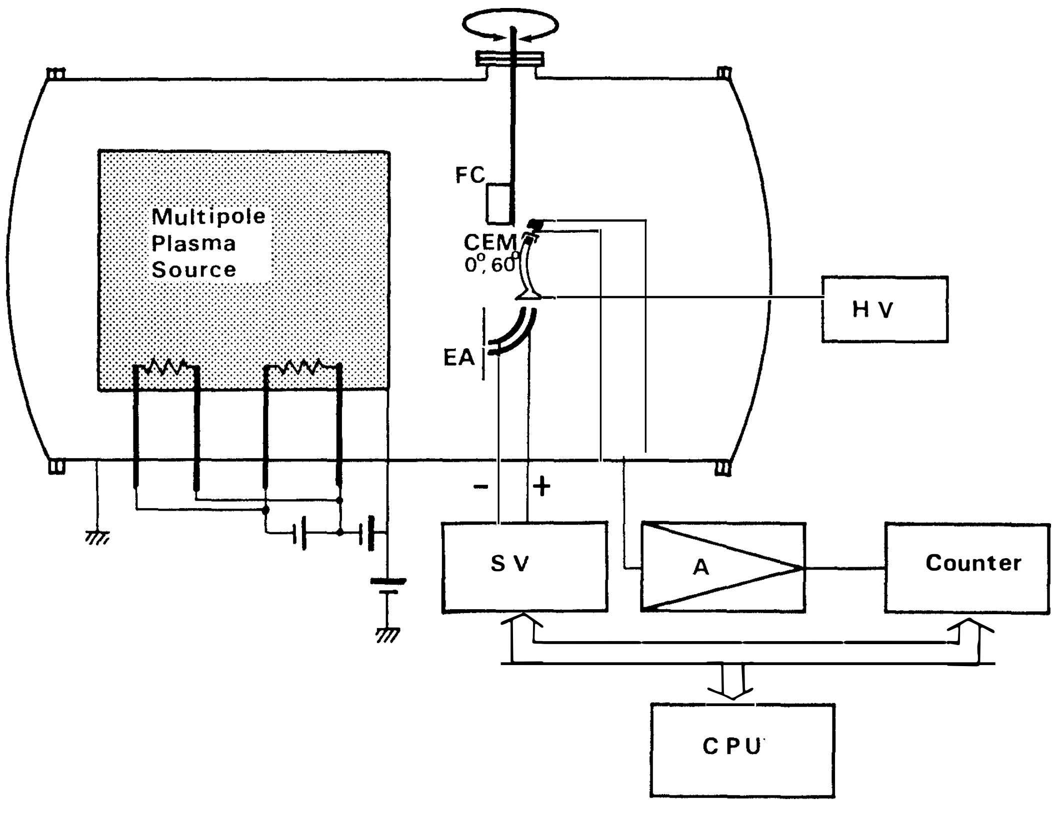


*Fig. 1. Setup of the experiment is shown schematically. The vaccum chamber is 2 m in length and 1 m in diameter. ESA and FC (Faraday Cup) are mounted so as to be able to rotate horizontally. Argon gas is introduced into the chamber for producing the argon plasma.*

tion efficiency by electrons emitted from heaters. While the number density of plasma inside the cage is of the order of magnitude of $10^{10}/cm^3$, the outward steady flow of the plasma from the cage makes the MPS device suitable as a source of the quiet plasma having the number density of about $10^5/cm^3$ at the ESA position.

Figure 2 depicts an example of the counts *vs.* energy diagram obtained by this setup. The vertical axis indicates the logarithm of counts per 10 ms, and the horizontal axis is the voltage applied to the ESA, which indicates 1/8th of the energy selected by the ESA. A steep rise of the curve shown near 0.6 V (*i.e.*, 4.8 eV of the energy selected by the ESA) corresponds to the plasma potential relative to the chamber wall. Figure 3 shows the energy distribution function ($f(E')$) calculated from Fig. 2

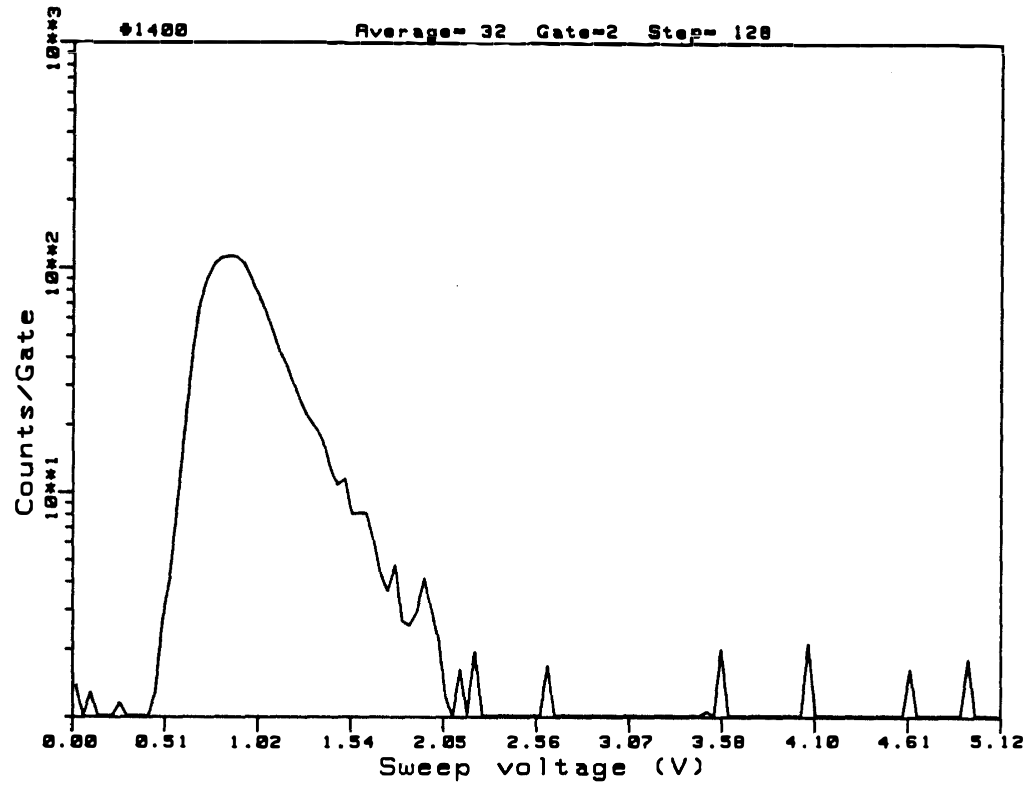


*Fig. 2. Counts vs. energy diagram obtained with the ESA. Vertical axis is the logarithm of counts detected by CEM in 10 ms, and horizontal axis is the voltage applied to the ESA which is one-eighth of the selected energy. Azimuthal angle of the ESA's view direction is +5°.*

by using eqs. (1) and (3). The curve in the figure falls off linearly in this logarithmic plot beyond 5 eV in accordance with the Maxwell-Boltzman distribution. Because, as noted before, eq. (1) is not valid over the entire energy range of the measurements, so it is difficult from this single spectrum to determine various parameters of the plasma. But the ion temperature can be estimated from this fall-off to be about 14000 K. This high temperature is understood by the fact that the mean free path of ions before colliding with neutral particles is much larger than the size of the vaccum chamber used in the experiment. This results in ions to be cooled insufficiently by neutral particles. On the other hand, due to the high plasma number density inside the cage, ions can make ample collisions with ions enough to have the Maxwell-Boltzman dis-

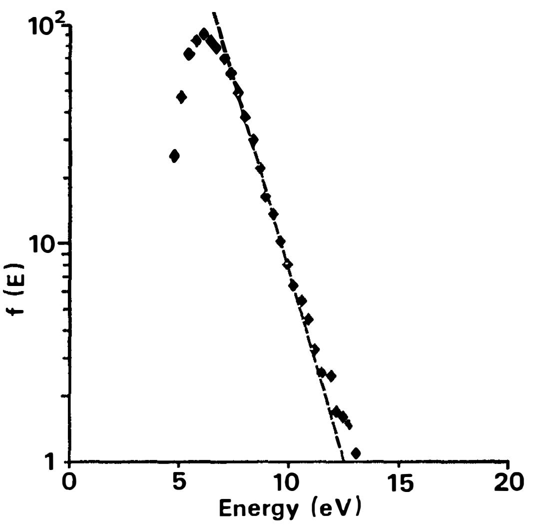


*Fig. 3.* *Energy distribution function calculated from Fig. 2 by using eqs. (1) and (3). Vertical axis is the $f(E)$ in arbitrary scale, and horizontal axis is the energy measured at the ESA. Plasma potential is not subtracted from the energy. Broken line indicates a exponential fit to the data.*

tribution function.

By rotating the ESA horizontally, we studied the angular dependence of distribution functions to be very complicated and far from a uniform distribution. This non-uniformity may be produced by the MPS device from which the plasma pours away through narrow slits at its wall. Figure 4 shows the counts *vs.* energy obtained at 20° of the azimuth angle, where 0° is defined as the ESA directed to the center of the

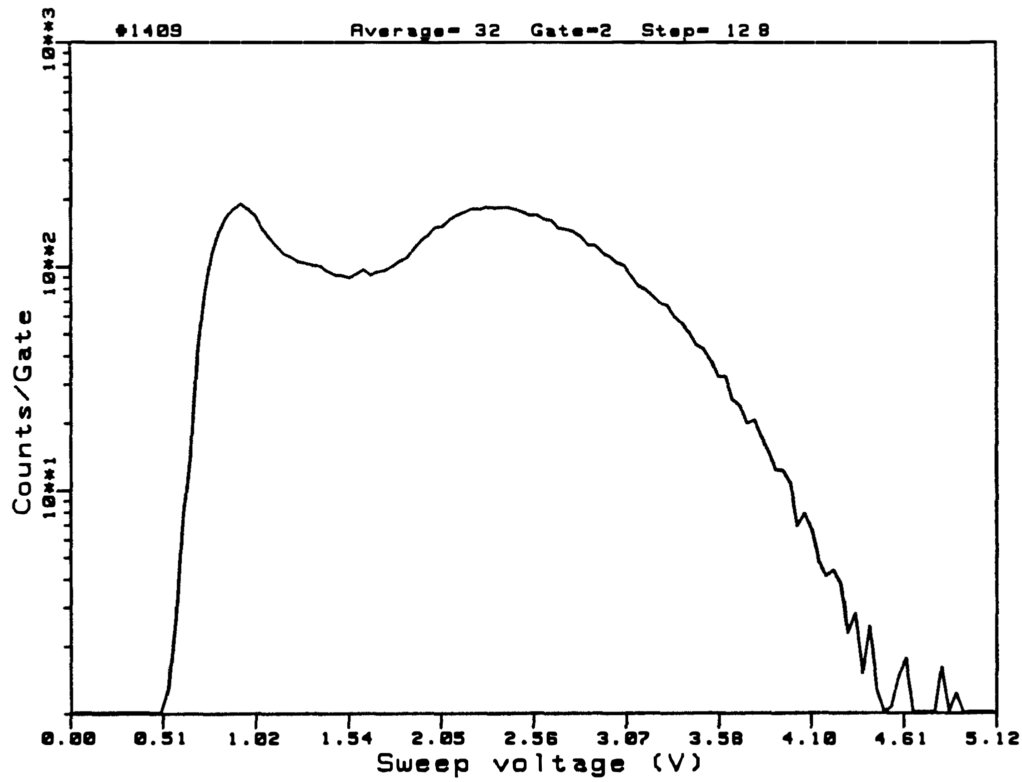


*Fig. 4.* *Same as Fig. 2 except azimuthal angle of —20°.*

MPS. The distribution function of this figure is shown in Fig. 5. The figure clearly indicates that the plasma has two components; one in the lower energy part similar to that shown in Fig. 3, another in the higher energy part. Long and short broken lines in the figure indicate these two components in the low and high energy parts, respectively. The figure shows the existence of an ion beam with the energy about 14 eV. Several counts *vs.* energy diagrams measured at different azimuthal angles are used to construct the countours of constant flux as shown in Fig. 6. Ordinate

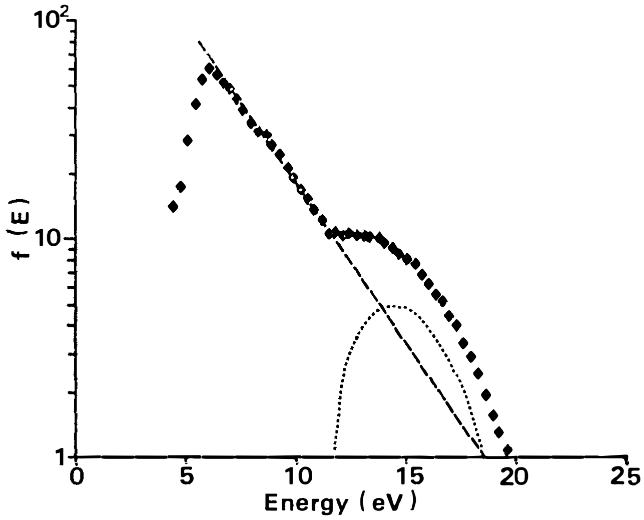


*Fig. 5. Energy distribution function calculated from Fig. 4. Short broken line indicates the high energy component of the distribution function, which is obtained by subtracting the long broken line from the data.*

and abscissa are ion velocities parallel and perpendicular to the 0° azimuthal angle. The figure also gives the arrangement of the sensor and MPS device. By scanning the azimuthal angle, the ESA detects ions coming from various parts of the MPS device, due to the large mean free path outside the cage. The contours clearly show that the higher energy part, or ion beam, is enhanced when the sensor gets sight of the heaters of the MSP located around ±20° of azimuthal angles. Then it is considered that the high energy ions are produced in regions near heaters and reach the ESA directly. Because this figure shows that eq. (4) cannot be applied directly in the case of our laboratory experiment, we have not tried to develop a computer program for fitting the data to eq. (4) to obtain the plasma parameters. But this should be done in the future analysis of the sounding rocket data.

It has been discussed extensively that contamination of the electrode surface which contacts directly with the ambient plasma causes distortions in the current-voltage characteristics of the plasma when voltage applied to this surface is swept as in the case of Langmuir probe. On the other hand, electrodes of the ESA to which sweep voltage is applied do not have a direct contact with the ambient plasma. This may make the ESA free from distortion of the energy spectrum. By applying the sweeping voltage so as to increase the selection energy or to decrease it, or by changing the scanning speed, we have observed the energy spectrum not to show any meaningful

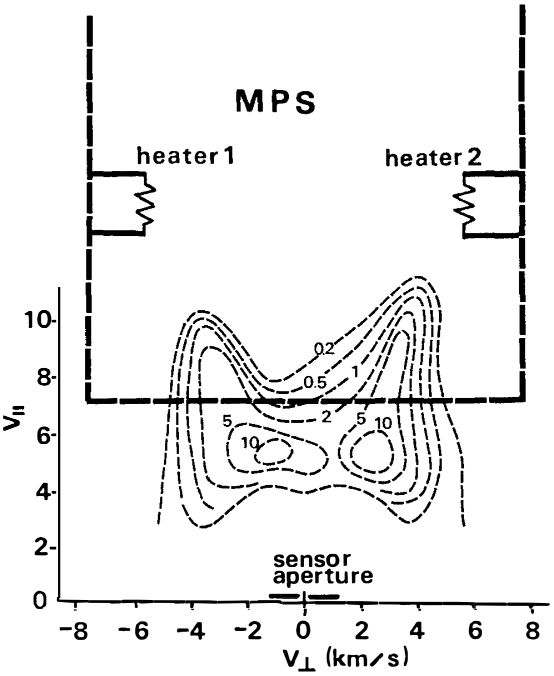


*Fig. 6. Contours of constant flux. Also shown is arrangement of the ESA and MPS. Numbers attached to contour lines are directional differential fluxes is arbitrary scale. Vertical and horizontal axes are velocities of ions parallel and perpendicular to the 0° azimuthal angle, respectively.*

change.

In summary of the experiment, the ESA is very capable of measuring the ion distribution functions in an energy range below 10 eV. It is also interesting that the ion distribution functions of the laboratory plasma are very complicated.

## 4. Instrumentation for a Sounding Rocket Experiment

The polar ionosphere is a suitable target for the measurements of the 3-D ion distribution functions by a sounding rocket because of several reasons. One, phenomena occurring in this region have not been fully understood due to the complicated ionosphere-magnetosphere coupling. Second, a sounding rocket which flies in the polar ionosphere along the trajectory close to the local geomagnetic field makes it easy to obtain the plasma drift velocity perpendicular to the field line by utilizing the rocket spin. Third, the electric field which causes the plasma drift is strong enough to be detectable in the polar ionosphere by this technique. Basic considerations of the rocket-borne instrument are described in the following sections.

### 4.1. Geometrical factor

Assuming the following conditions; plasma number density of $10^6$/cm$^3$, ion temperature of 1000 K, $V_0$ of 1 km/s, $\Delta U$ of 1 V, and mean ion mass of 16 amu, we can estimate the maximum incoming flux into the ESA to be about $10^{12}$/cm$^2$ sr s eV by using eq. (4) (MORGAN and ARNOLDY, 1978). Restriction imposed on the counting rate to be less than about $10^7$/s results in a geometrical factor less than $10^{-5}$ cm$^2$ sr eV/eV. The ESA with this value of the geometrical factor can be easily accommodated to the small sounding rocket.

### 4.2. *ESA*

There are several types of the ESA currently available for the sounding rocket experiment. In order to make the 3-D measurements during one rocket spin period, the instrument should view in multiple, at least two, directions simultaneously. This can be achieved by using several ESA's or a single quadrispherical ESA with multiple CEM's. The number of view directions and the type of the ESA will be limited by resources available in the rocket such as telemetry speed, weight and volume.

The entrance aperture of the ESA should be surrounded with a large and flat conductive surface in order to make the sheath electric field uniform. If the size of this surface is much larger than the sheath thickness, we can neglect particle acceleration parallel to this surface.

### 4.3. *Ion mass analysis*

The mean ion mass of the ionosphere in the $F$ layer varies from 30 ($NO^+$) to 16 ($O^+$) with increasing altitudes. Because the mean ion mass should be provided externally in the data analysis, this is better to be measured simultaneously than taken from the model ionosphere. The instrument for this purpose needs not be a sophisticated one which has been used in the detailed mass analysis in the ionosphere but be able to discriminate $O^+$ from $NO^+$ and $O_2{}^+$. Therefore, a simple type of ion mass spectrometer such as a small magnetic sector or a time-of-fligh instrument will work well.

## Acknowledgments

Quadrispherical electrostatic analyzer used in the experiment has been kindly provided by T. MUKAI at ISAS.

## References

GREEN, D. W. and WHALEN, B. A. (1974): Ionospheric ion flow velocities from measurements of the ion distribution function technique. J. Geophys. Res., **79**, 2829–2834.

HANSON, W. B. and HEELIS, R. A. (1975): Techniques for measuring bulk gas motions from the satellites. Space Sci. Instrum., **1**, 493–517.

MORGAN, B. G. and ARNOLDY, R. L. (1978): A determination of $F$ region electric fields from rocket measurements of ionospheric thermal ion spectra. J. Geophys. Res., **83**, 1055–1061.

WHALEN, B. A., GREEN, D. W. and MCDIARMID, I. B. (1974): Observations of ionospheric ion flow and related convective electric fields in and near an auroral arc. J. Geophys. Res., **79**, 2835–2842.

ZANETTI, L. J., Jr., ARNOLDY, R. L., CAHILL, L. J., Jr., BEHM, D. A. and GREENWALD, R. A. (1980): Comparative rocket observations of ionospheric electric fields in the auroral oval. Space Sci. Instrum., **5**, 183–196.

*(Received May 17, 1984; Revised manuscript received December 12, 1984)*